

# Design Compact Antenna for Energy Harvesting Application

Reham Mahmood Yaseen<sup>1</sup>, Dhirgham Kamal Naji<sup>2</sup>

Electronic and Communications Engineering Department, College of Engineering,

Al-Nahrain University, Baghdad, Iraq

**ABSTRACT:** This paper proposes a new design approach of two dipole antennas operating at 2.45 GHz for energy harvesting application. The first designed antenna is a patch antenna (PA) and its complementary structure, slot antenna (SA), is the second design. The proposed two antennas having a radiating structure comprising of three elements: meander line, spiral and folded dipole structures as strips and slots printed in FR4 substrate for PA and SA, respectively. The proposed antennas are characterized by small sizes  $28 \times 10 \times 0.8 \text{ mm}^3$ , simple structures and having an input impedance easily conjugately matched with impedance of the rectifier. The interaction between the three radiating parts makes the proposed PA and SA having a 3dB impedance bandwidth of 50 MHz and 60 MHz covering 2.39–2.44 GHz and 2.39–2.45 GHz bands, respectively. Simulated and measured results of input impedance of the proposed PA and SA are closely similar making them suitable to be used for energy harvesting applications.

**Index Terms**— Energy harvesting, Folded dipole, Impedance matching, Meander, Spiral.

## 1 INTRODUCTION

Lately, antenna with energy harvesting capability has been receiving enormous interests especially energy, that is in form of radio frequency (RF) ambient signals. These signals, whether deployed outside or inside the open air, their ability makes it the optimum choice as the energy to be harvested considering its continuous operation thus preferable to be then developed for self-sustain technologies [1]. In RFID system the antenna is an important part. The reader's antenna plays a most important role in the overall RFID system performance factors, such as the overall size, the reading range, and the compatibility with tagged objects. The design goal is to achieve multiband resonance frequency, and to miniaturize the antenna size. The great challenging problem that restricts the antenna performance is antenna miniaturization because of a physical fundamental limit for small antennas [2].

There have been many researches which aimed to reduce the size of antenna and improve the antenna efficiency. In reference [3], design and implantation an antenna with input power ranging from  $-20$  to  $0 \text{ dBm}$ . To obtain the maximum PCE, our investigation displays that the optimal rectenna structure should not only optimize those design factors however also eliminate the matching circuit between an antenna and a rectifier for ultralow-power scenarios. The consequent PCE at 2.45 GHz is 61.4% and 31.8% at  $-5$  and  $-15 \text{ dBm}$ , respectively. In reference [4], a design and implantation a high-efficiency 2.45-GHz antenna that can harvest low input RF power effectively. A new antenna with a simple structure and high gain of 8.6 dBi is proposed for

the rectenna. The overall efficiency of the proposed antenna can achieve 80.3% and 50% with power density of 1.95 and 0.22 W/cm, respectively. In reference [5] design and implantation a 2.45 GHz antenna consisting of an adjusted Vivaldi antenna with a broadside radiation and a half-wave series voltage multiplier. It set of a 5-stage voltage multiplier connected to a Vivaldi antenna modified in order to obtain a broadside radiation. The operation distance of about 70 cm is wanted when the transmitted power is set at 130 mW. In reference [6] presented novel approach to designing antenna systems by eliminating the use of a matching network between the antenna and the rectifier is presented. The proposed antenna consists of a wide impedance bandwidth 8 octagon disks placed at two different layers laying on both sides of a single substrate and backed by a ground plane. The measurement results of the antenna introduce a 50% radiation to DC efficiency at the operating frequency of 2.1 GHz.

Various designs of the antenna have been reported, that is, covered slot antenna [7], circular patch antenna [8], meander antenna [9], planar inverted F-antenna [10], folded dipole antenna [11], and so on. Moreover, many impedance matching techniques including slot structure [12], T-matching structure [13], inductively/capacitive coupled structure [14,15], have been developed. But, a major challenge is to reduce the overall sizes of these advanced.

## 2 DESIGN ANTENNA

The simulated model of the proposed antenna is shown in Fig. 1(a-b). It is printed on FR4 substrate with thickness 0.8 mm and relative permittivity  $\epsilon_r = 4.3$ . The patch and slot of antenna are printed meander with the spiral and folded dipole with  $kt_i = 0.07$  when  $i=1,2,\dots,6$  and  $kd_1 = 0.4$ ,  $kd_2 = 0.4$  and  $kd_4 = 0.4$  while  $kd_3, kd_6, kd_7, kd_8, kd_9$  and  $kd_{10} = (1/13)$  and  $kd_5 = 0.6/13$  when  $kl_3 = 0.5$  table illustrate the values of antenna parameter at the working frequency.

TABLE 1

THE VALUES OF RECTENNAS PARAMETERS

Parameters	Value	Equation
$W_{sub}$	40	-
$L_{sub}$	14	-
$d_i$	-	$d_i = kd_i \left( \frac{W_{sub}}{2} - \frac{L_1}{2} - L_2 - 8t \right)$ $i = 1, 2, \dots, 10$
$t_i$	0.7	$t_i = (L_{sub} - 8t)kt_i$ $i = 1, 2, \dots, 6$
$L_1$	4	$L_1 = (L_{sub} - 8t_p)(kt_1 + kt_2 + kt_3 + kl_3) + 4t_p$
$L_2$	3	-
$W_1$	4	-
$W_2$	0.5	-
$t_p$	0.3	-
$T$	0.035	-

Fig.2 shows the comparison between the return loss of patch and slot antennas. As observed from Fig.1, the return loss for slot antenna and patch rectenna.

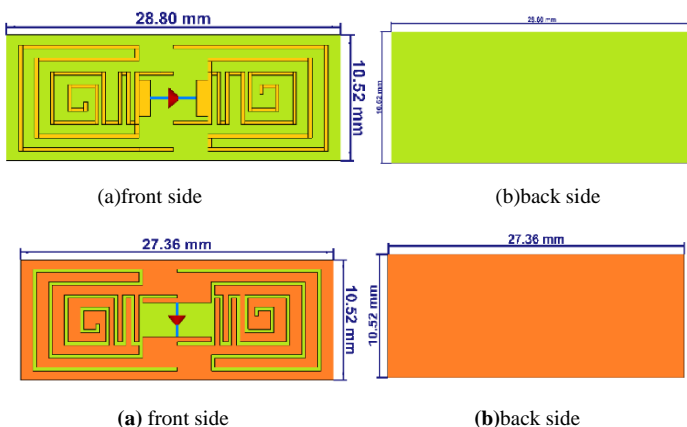


Figure 1 shows the proposed (a) patch antenna (b) slot antenna

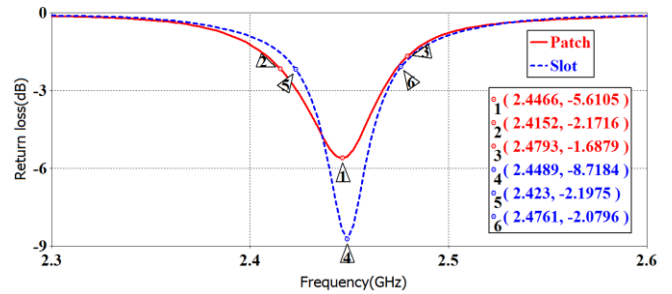


Figure 2 shows the return loss of patch and slot antennas.

Fig3(a-b) this figure presents the simulated impedance matching (real and imaginary) for both patch and slot antennas. Impedance matching for patch antenna (real part) is 19.11 ohms and imaginary part is 169.02 and impedance matching for slot antenna (real part) is 12.853 ohms and imaginary part is 168.81.

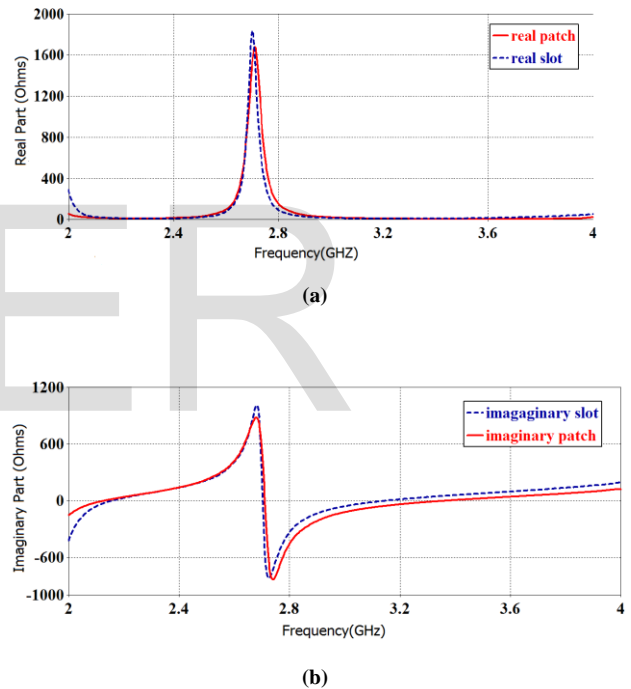


Figure 3 The simulated input impedance for PA and SA. (a) Real part. (b) Imaginary part.

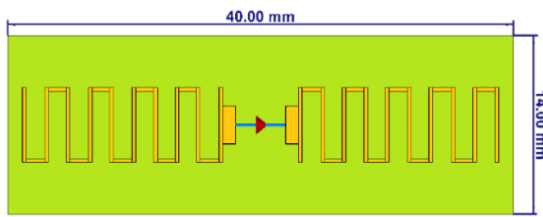
## 3 Evaluation design steps of the proposed patch antenna

Four design steps besides the working principle of the proposed patch rectenna are presented in this section.

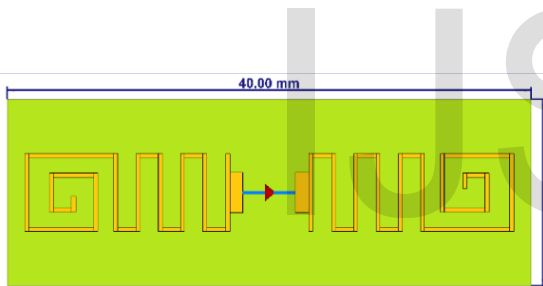
In the first step the meander line antenna is printed on the front side of FR4 substrate with dimensions length and width are (14mm × 40mm) respectively. While the second step is designed by adding spiral antenna to the end of meander line that designed in the first step. In the third step of designed procedure, a meander line antenna with end spiral and double folded dipole is designed. In the final step of designed

procedure, the proposed antenna is designed from step three by increasing the first width and decreasing the second width of meander line by ( $d_3$  and  $d_2$ ) respectively and the total dimensions of substrate is decreased by ( $28.8mm \times 10.52mm$ ).

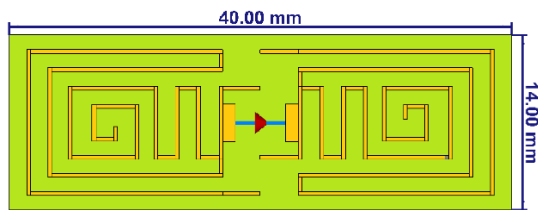
As shown in Fig. 4e the return loss for patch0 and patch1 is nearly 2.4 GHz for -3dB VSWR so that spiral antenna is added to the end of meander line and in Fig. 4e the return loss for patch2 is 2.8 GHz for -3dB so that double folded dipole is designed. The proposed rectenna (patch3) operates at the desired frequency response (2.446GHz for -3dB VSWR) after miniaturized size as shown in Fig.4d.



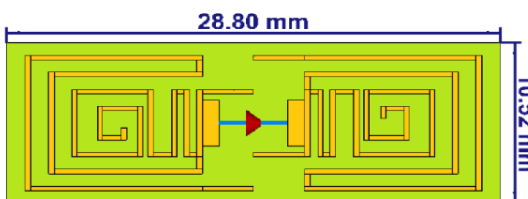
(a) meander line antenna (patch0)



(b) meander line with end spiral and (patch1)



(c) meander line with end spiral and double folded (patch2)



(d) proposed antenna (patch3).

Figure 4e The comparison between the return loss of the four shapes of patch antenna.

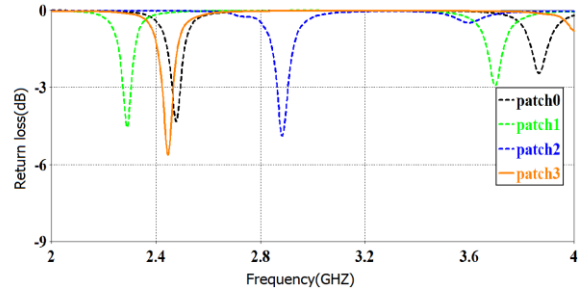


Figure 4e The comparison between the return loss of the four shapes of patch antenna.

### 4 Performance Result of the Proposed Patch Antenna

This section describes the performance results of the proposed patch antenna radiation pattern 3D and 2D.

Fig. 5 and Fig. 6(a-b) and Fig.7(a-b) shows the simulated 3D and (a-b) 2D radiation pattern (when  $\phi = 90$  and  $\phi = 0$ ) and (a-b) 2D radiation pattern (when  $\theta = 90$  and  $\theta = 0$ ) respectively. The proposed patch antenna shows omnidirectional 3D radiation at the operating frequency band (2.42 GHz). While the 2D radiation pattern for patch antenna for both values of  $\phi$  (90 and zero degree) are nearly bidirectional radiation at the desired frequency response 2.42 GHz.

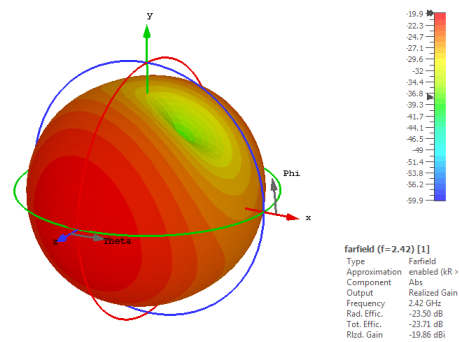


Figure 5 3D radiation pattern for patch antenna.

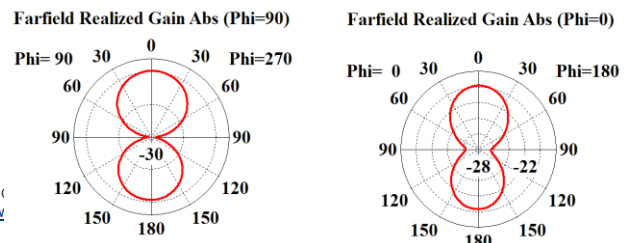


Figure 6 2D radiation pattern for (a) Phi =90 (b) Phi =0.

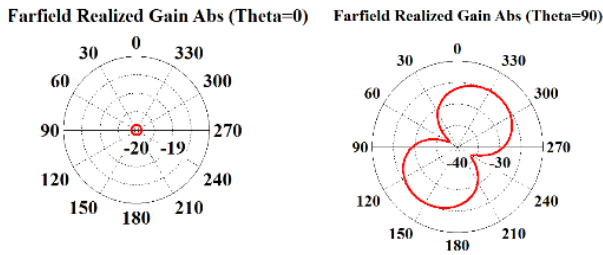


Figure 7 2D radiation pattern for (a) theta =90 (b) theta =0.

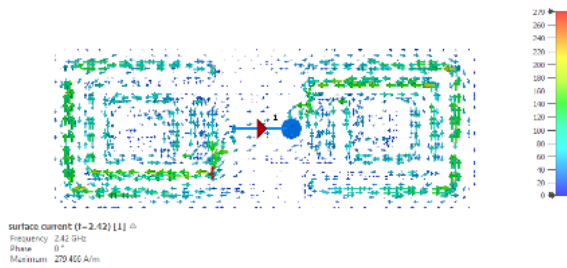


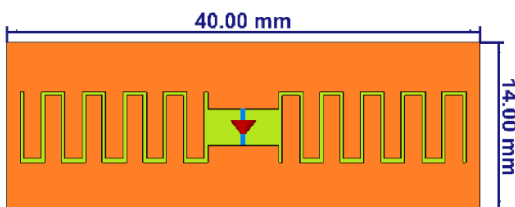
Figure8 shows the surface current for patch rectenna.

### 5 Evaluation design steps of the proposed slot antenna

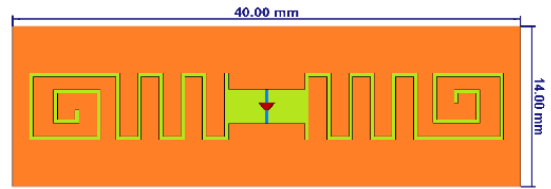
Four design steps besides the working principle of the proposed slot antenna are presented in this section.

In the first step the meander line antenna is printed on the front side of FR4 substrate with dimensions length and width are (14mm × 40mm) respectively. While the second step is designed by adding spiral antenna to the end of meander line that designed in the first step. In the third step of designed procedure, a meander line antenna with end spiral and double folded dipole is designed. In the final step of designed procedure, the proposed antenna is designed from step three by increasing the first width and decreasing the second width of meander line by ( $d_3$  and  $d_2$ ) respectively and the total dimensions of substrate is decreased by (27.36mm × 10.52mm).

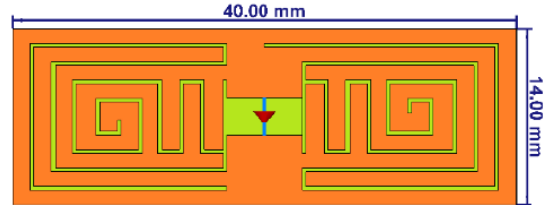
As shown in Fig.9 (e) return loss for slot0 is nearly 3.2 GHz for -3dB VSWR so that spiral antenna is added to the end of meander line the return loss in fig.9(e) for slot1 is nearly 2.2 GHz for -1 dB and in Fig. 10-c the return loss for slot2 is 2.8 GHz for -3dB so that double folded dipole is designed. The proposed antenna (patch3) in Fig. 9(d) operates at the desired frequency response (2.448 GHz for -9dB VSWR) after miniaturized size.



(a)meander line antenna(slot0)



(b)meander with spiral(slot1)



(c)meander with spiral and folded dipole.

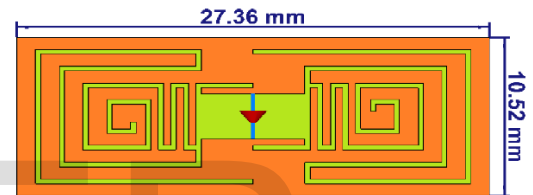


Figure 9-d proposed antenna(slot3).

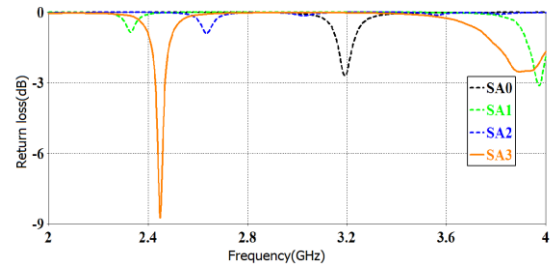
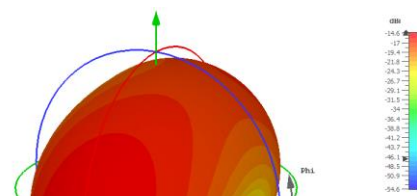


Figure 9e The return loss of the four shapes.

### 6 performance result of the proposed slot antenna

The section shows performance result of slot antenna radiation pattern (2D and 3D radiation). Figures 10, 11 and 12 show the simulated 3D and 2D radiation pattern, respectively. The proposed SA shows omnidirectional 3D radiation at the operating frequency band (2.42GHz). While the 2D radiation pattern for SA for both values of phi (90) and zero degree are nearly bidirectional radiation at the desired frequency of 2.42 GHz.



the rectenna is characterized using network parameters as [16].

$$Z_{in} = \frac{2Z_o(1 - S_{11}S_{22} + S_{12}S_{21} - S_{12} - S_{21})}{(1 - S_{11})(1 - S_{22}) - S_{12}S_{21}}$$

Here,  $Z_o$  is the characteristic impedance of the connected transmission lines, which is 6-j170 for most of measurement systems. Figure 15 shows the fabricated transmission line used to connect between Agilent E5071C vector network analyzer and the antenna. Figure 16 shows the measured input impedance which is in a good agreement with the simulated results. It can be seen that the input impedance of the patch antenna is 19+j165 at 2.50041GHz and the input impedance of the slot antenna is 12+j175 at 2.426GHz.

Figure10 3D radiation pattern for slot antenna.

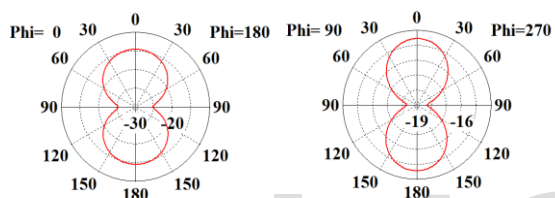


Figure11 2D radiation pattern for slot antenna (a) phi=90 (b) phi =0

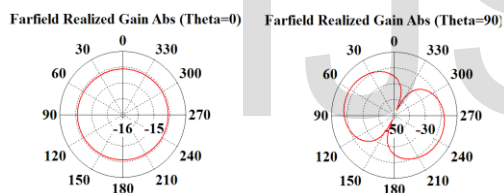


Figure 12 2D radiation pattern for slot antenna (a) theta=90 (b) theta =0

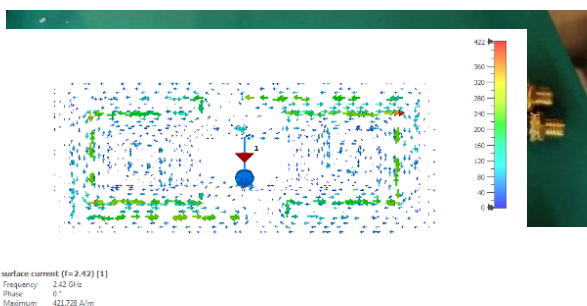


Figure 13 The surface current of the slot antenna.

## 7 Measured results

The proposed patch and slot antennas are fabricated and studied, as shown in Figure 14(a-b). The antenna can be considered as a two-port network and the impedance of

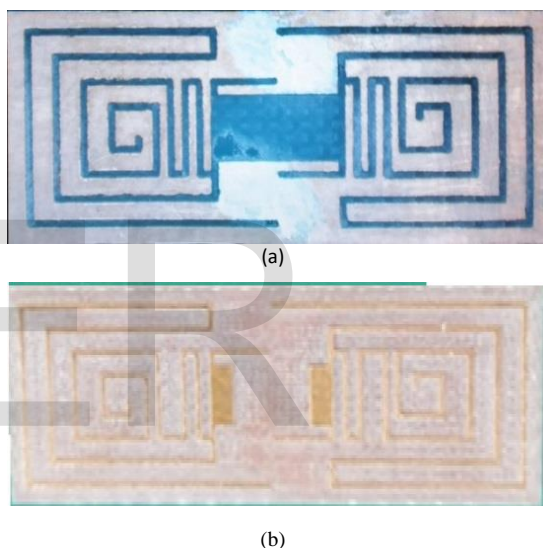
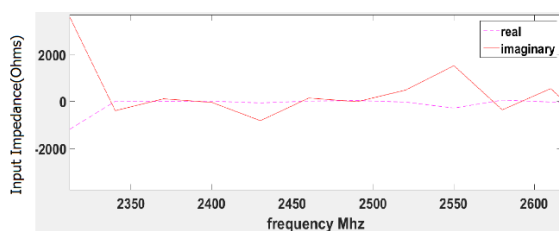
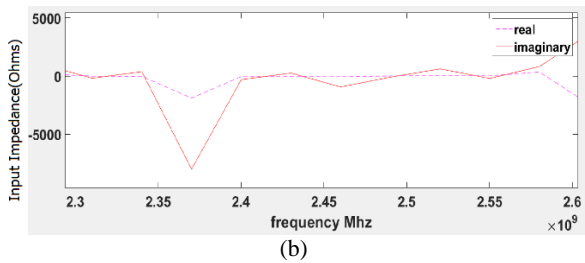


Figure 14 Photograph of antenna (a) patch antenna (PA) (b) slot antenna (SA).

Figure 15 The connected transmission line for impedance measurement.



(a)



**Figure 16** Measured input impedance of the fabricated antennas (a) patch antenna (b) slot antenna.

**TABLE 2**

**COMPARISON BETWEEN ANTENNA SINGLE BAND**

Reference	Frequency(G Hz)	Use of impedanc e matching networks	Physical size (WsubxLsub)	Substrate, Dielectric Constant, Thickness(mm )	Antenna type
[3]	2.45	No	50 X 40mm <sup>2</sup> 70 X 60mm <sup>2</sup>	FR4 $\epsilon_r = 4,4$ $h_{sub} = 0,8$	Patch and Quasi-Yagi antenna
[4]	2.45	No	110 X 90mm <sup>2</sup>	RT/Duroid600 2 $\epsilon_r = 2,94$ $h_{sub} = 25$	Coplanar antenna
[5]	2.45	Yes	76.8 X76mm <sup>2</sup>	FR4 $\epsilon_r = 3,9$ $h_{sub} = 1,6$	Vivaldi antenna
[6]	2.2	No	71 X 71mm <sup>2</sup>	RT/Doroid588 ORogers $\epsilon_r = 3,9$ $h_{sub} = 1,6$	Octagonal antenna
This work	2.45	No	27.36 X 10.52mm <sup>2</sup> 28.8 X 10.52mm <sup>2</sup>	FR4 $\epsilon_r = 4,3$ $h_{sub} = 0,8$	Slot antenna Patch antenna

AS can be seen in the table above, the peoposed antenna achieved the smallest size in the comparison with [3] to [6]. The antenna in [4] has the largest size but the design is complex with multi-layer materials, so this is considered as a disadvantage in terms of the design. The proposed antenna is the simplest in the design and has the smallest size.

**8 CONCLUSIONS**

This paper proposes a compact design of antennas composed of mender line, spiral and folded dipole structures. The proposed antennas are of a small sizes for PA and SA as  $28 \times 10 \times 0.8 \text{ mm}^3$  with broad bandwidth covering 2.39–2.44 GHz for PA and 2.39-2.45 GHz for SA. The proposed PA operates at 2.446 GHz with return loss (-5.6257 dB) and

bandwidth 50 MHz and SA works at at 2.4483 GHz with return loss (-8.6393 dB) and bandwidth 60 MHz. The measured input impedance of PA and SA are  $19+j165$  at 2.5 GHz and  $12+j175$  at 2.426 GHz, respectively which are in agood agreement with the simulated results.

**REFERENCES**

[1] Kuhn V, Lahuec C, Seguin F, Person C. A, "multi-band stacked RF energy harvester with RF-to-DC efficiency up to 84%," *IEEE Trans. Microw. Theory Tech.*, Vol. 63, No. 5, 1768-1778, 2015.

[2] RFIDEA: Engineering & Applications in electronic traceability.

[3] Yen- Chen and Cheng-Wie Chiu. " Maximum achievable power conversion efficiency obtained through an optimized rectenna structure for RF energy harvesting," *IEEE Transactions on antennas and Propagations*, Vol.65, No 5. 2017.

[4] Hucheng Sun, Yong-xin Guo, Miao He, and Zheng Zhong, "Design of a high-efficiency 2.45- GHz rectenna for low-input-power energy harvesting," *IEEE Antennas Wireless Propag. Lett.*, vol. 11, pp. 929–932, 2012.

[5] Fobrizio Congedo, Giuseppina Monti, Luciano Tarricone and Valter Bella. " A 2.45-GHz vivaldi rectenna for the remote activation of an end device radio node". *IEEE Sensors Journal*.VOL 13. No.9. 2013.

[6] Thamer S. Almoneef. "Design of a Rectenna Array Without a Matching Network," *IEEE Access*. 2020.

[7] Mohamed M. Mansour and Haruichi Kanaya. "Novel L-Slot Matching Integrated with Circularly polarized Rectenna for wireless Energy Harvesting", 2019.

[8] Shanpu shen, Chi-Yuk Chiu and Ross D. Murch. "A dual-port triple-band L-probe microstrip patch rectenna for ambient RF energy harvesting," *IEEE Antennas and wireless propagation Letters*, Vol. 16, 2017.

[9] Kayan Celik and Erol Kurt., " A novel meander line integrated E-shaped rectenna for energy harvesting applications". *Wiley International Journal of RF and Microwave Computer-aided Engineering*, 2018.

[10] F. N. M. Redzwan, M.T. Ali, M.N. Md. Tan, and NF. Miswadi, " Design of Planar Inverted F Antenna for LTE Mobile Phone Application," 2014.

[11] Fang Zhang, Xin Liu, Fan-Yi Meng, Qun Wu and Nam-Young Kim. "Design of a Compact Planer Rectenna for Wireless Power Transfer in the ISM Band," *International Journal of Antennas and Propagation*, 2013.

[12] G. Marrocco." The art of UHF RFID antenna design: Impedancematching and size-reduction techniques". *IEEE Antenna Propag Mag* 50, 66–79. 2008.

[13] A. A. Sharatol Ahmad Shah, N. H. Abd Rahman and M. T. Ali "Design of Electro-Textile UHF RFID Tag through T-Match Network," *IEEE International RF and Microwave Conference*, 2018.

[14] Fei Lu, Hua Zhang, Heath Hofmann and Chris Mi, "An Inductive and Capacitive Integrated Coupler and Its LCL Compensation Circuit Design for Wireless Power Transfer," *IEEE*, 2016.

[15] Jiejian Dai and Daniel C Ludois, "A Survey of Wireless Power Transfer and a Critical Comparison of Inductive and Capacitive Coupling for Small Gap Applications," *IEEE Transactions on Power Electronics*, vol. 30, pp. 6017-6029, 2015.

[16] Xianming. Qing, Chean Khan Goh, and Zhi Ning Chen. "Impedance characterization of RFID tag antennas and application in tag co-design," *IEEE Trans Microwave Theory Tech*, Vol. 57, 1268–1274, 2009.

IJSER